Sonochemical-Assisted Synthesis of a Novel Nano-Cobalt(II) Coordination Complex Toward Morphology Design, and Control: Crystallography and Hirshfeld Surface Analysis Studies

Abdollahi, Noshin
Department of Environmental Engineering, College of Engineering, Hamedan Branch, Islamic Azad University, Hamedan, I.R. IRAN

Jalilzadeh Yengejeh, Reza *[*+]*
Department of Environmental Engineering, Ahvaz Branch, Islamic Azad University, Ahvaz, I.R. IRAN

Goodarzi, Amir Reza
Department of Civil Engineering, College of Engineering, Hamedan Branch, Islamic Azad University, Hamedan, I.R. IRAN

Sobhan Ardakani, Soheil
Department of the Environment, College of Basic Sciences, Hamedan Branch, Islamic Azad University, Hamedan, I.R. IRAN

Payam Hayati
Organic and Nano Group, Department of Chemistry, Iran University of Science and Technology, Tehran, I.R. IRAN

ABSTRACT: *Nano-structures of Cobalt Metal-Organic Complex (Co-MOC), $[Co(NCS)_2(L)(H_2O)_2.3(L)]$ {1} (L=2,5-dimethyl pyrazine), have been synthesized under different experimental conditions. Micrometric crystals (bulk) or nano-sized materials have been obtained depending on using the branch tube method or sonochemical irradiation. All materials have been characterized by Scanning Electron Microscopy (SEM), Powder X-Ray Diffraction (PXRD), FT-IR spectroscopy, and elemental analyses. Single crystal X-ray analyses on **1** display that Co^{2+} ions are 6-coordinated and 0D coordination complex and two organic ligands (L) are not coordinated to Co(II) in the crystal lattice. Moreover, the impacts of the following parameters were investigated: ultrasonic power, reaction temperature, and reactant concentrations on structural and morphological features of the obtained materials. In the following step, the size of the nanomaterials was investigated based on SEM images. Finally, the intermolecular interaction of molecular crystals of 1 was also studied by Hirshfeld surface analysis.*

KEYWORDS: *Nano-shaped; Metal-Organic Complex; Ultrasonic; Hirshfeld surface analysis.*

*****To whom correspondence should be addressed.*
+ *E-mail: r.jalilzadeh@iauahvaz.ac.ir*
1021-9986/2023/9/2834-2844 11/$/6.01

INTRODUCTION

In recent decades, one of the major scientific concerns has been designing and fabricating novel self-assembled supramolecular metal-organic coordination complexes (MOC) with fascinating structures and topologies. In this respect, enormous efforts have been focused on the design of coordination complexes with various metal and organic ligands leading to emerging a large variety of MOCs with various potential applications such as adsorption, catalysis, magnetism, luminescence, nonlinear optics, and molecular sensing [1-15].

Within the structure of this type of material, various types of strong and weak chemical interactions play roles in complex structure assembling. For example, connecting metal ions to organic linkers via a strong coordination bond and weak interactions such as hydrogen bonding and π–π stacking [16–18]. Therefore, the choice of appropriate organic ligands is a key factor to adjust the final structures of complexes [19–21]. Also, cobalt as an abundant earth - 3d metal is a suitable choice to construct MOCs due to its availability, lower cost, and low toxicity [22]. To achieve MOCs, several different techniques have been developed including a) slow diffusion b) evaporation, c) precipitation/recrystallization d) hydrothermal, and e) sonochemical method [23]. Also, in recent years, a vast diversity of nano-shaped MOCs has been produced using various techniques, such as precipitation, microemulsion, solvothermal techniques, microwave-assisted as well as sonochemical methods [24,25]. The sonochemical method is promising regarding its advantages over other methods such as requiring low reaction times, temperature, and pressures and more importantly, it's a more useful method to produce nanoscale particles and now it's been proven to be a powerful method to produce nano-sized metal-organic complexes [26–33]. The sonochemical technique by applying high-energy sound waves can start a process through bubbles that are produced and collapsed in an aqueous medium [34], therefore, a variety of reactions can be initiated using this technique [35–37].

However, sonochemical methods have been adopted for the preparation of nanomaterials, and the application of the ultrasonic method for the construction of MOCs receives relatively limited attention. Until now, some examples of $(adH)_3[Co(Hpzdc)(pzdc)_2].6H_2O$ and $[Co(pzdc)_2(H_2O)_2]_n$ (where H_2pzdc is 2,3-pyrazinedicarboxylic acid and ad is adenine) [38], $\{[Co(L_2)(mip)]\cdot 0\cdot .5H_2O\}_n$, L_2 = 1,6-bis(benzimidazole)hexane, H_2mip = 5-methylisophthalic acid) [39], $[Co(Hbibp)(nbta)]_n$, (bibp = 4,4′-bis(1-imidazolyl)biphenyl, H_3nbta = 5-nitro-1,2,3-benzenetricarboxylic acid) [40], $[Co(NH_3)_6]Cl_3\cdot 2H_2O$, $[Co(en)_3]Cl_3\cdot 3H_2O$ (en-ethylenediamine), $[Co(dien)_2]Cl_3\cdot 3.5H_2O$ (dien-diethylenetriamine) [41], $[Co(dipic)(2,2'\text{-bipyridine})(H_2O)]_3 \times 10H_2O$, where $dipic^{2-}$ = pyridine-2,6-dicarboxylato [42], $[Co_2(ppda)(4\text{-bpdh})_2(NO_3)_2]_n$ (where, ppda = p-phenylenediacrylic acid, 4-bpdh = 2,5-bis(4-pyridyl)-3,4-diaza-2,4-hexadiene) [43], rare 0D Co(II) coordination complex with different ligand are reported. One, two and three-dimensional coordination polymer compounds have been synthesized more than zero-dimensional, and the design and synthesis of these types of zero-dimensional compounds should be more accurate. The study on morphology control in different conditions and the synthesis of nano-cobalt(II) complexes of these compounds has been done less. This current research tried to investigate these structures which have been less considered. However, the synthesis of cobalt-based 0D coordination complexes still represents a challenge. Herein, the synthesis of a novel MOC was reported. The impacts of sonochemical-related parameters including irradiation power, reaction temperature, and reactant concentration were assessed to reach desirable particle features. The characterizing instruments including SEM and PXRD were used to investigate the products.

Herein, we report the synthesis of a novel nanoscale 0D Co(II) coordination complex with the ultrasounds method. We will demonstrate that this is a robust process independent of experimental parameters such as irradiation power, reaction temperature, and reactant concentration. Moreover, crystals suitable for X-ray diffraction of the same complex have been obtained by the branched tube method and successfully compared with the X-ray diffraction of sonochemical samples. Finally, the interaction between molecules in crystal packing of **1** was discussed by Hirshfeld surface analysis.

EXPERIMENTAL SECTION

Materials and instruments

All used to-start materials were obtained from Sigma-Aldrich without further purification. FT-IR spectrophotometer was used for recording IRTracer-100 FT-IR (Shimadzu). Elemental analyses were recorded using the FlashEA 1112 series (model: Thermo Finnigan).

Table 1: Crystal data and structure refinements for compound 1

Formula	$C_{26}H_{36}CoN_{10}O_2S_2$
MW /g·mol^{-1}	643.70
Crystal system	triclinic
Space group	P_1–
a /Å	7.5112 (5)
b /Å	10.2924 (7)
c /Å	11.0063 (7)
α /°	92.666 (5)
β /°	107.268 (5)
γ /°	98.151 (5)
V /Å3	800.78 (9)
T /K	293
Z	1
*D*calc /Mg·m^3	1.335
μ /mm^{-1}	0.706
*θ*max /°	28.00
Refl. collected	12537
Unique reflections	3820
*R*int	0.0334
Refl. [*F*o >4σ(*F*o)]	3504
Parameters	191
*R*1 [*F*o >4σ(*F*o)]	0.0315
wR_2	0.0829
GOF	1.061
$\Delta\rho_{max/min}$ /e·Å^{-3}	0.294 / –0.235
CCDC No.	1543637

XRD measurements were conducted by Philips (model: PW1730). SEM images were obtained using Perseus Edu. Ultrasonic irradiation was applied by an Ultrasonic processor (Hielscher, up200H). The melting points were measured by electrothermal 9100 apparatus. Single-crystal X-ray diffraction analyses of **1** were performed using (EMMA) Enhanced Mini-Materials Analyser). SADABS program reduced the data and corrected semiempirical absorption [44]. SIR97 program was utilized to solve the structure [45] and refining was accomplished using the full-matrix least-squares method on F^2 utilizing the SHELXL-2016/6 program [46] with the aid of the WinGX program [47]. PLATON program was utilized to perform molecular graphics [48]. Hirshfeld surface analysis was performed using CrystalExplorer17 software [49]. Mercury software was operated to obtain simulated XRD patterns based on single crystal data [50].

Branched-tube synthesis of 1 as a single crystal

Briefly, 0.6 mmol $Co(NCS)_2$ and 7.2 mmol 2,5-dimethyl pyrazine (L) were mixed in water under 30 min stirring at room temperature followed by the insertion of $Cu(NO_3)_2.6H_2O$ (295 mg, 2 mmol) and, then, the final mixture was placed in a branched tube. Next, the sealed setup went under 60 °C heating for a week, as well as, then, the temperature was slowly decreased to ambient temperature leading to the production of black crystals of **1**. The SCXRD analysis of **1** was carried out after filtration and air-drying of the crystals at room temperature. Yield: 54%. $C_{26}H_{36}CoN_{10}O_2S_2$: calcd. C= 48.51, H =5.59, N =21.76, S =9.96%; found C =45.84, H =5.46, N =20.31, S =9.34%. IR (selected bands for 1; in cm^{-1}): 3365(b), 3151(b), 2089(w), 1630(s), 1593(s), 1565(s) [51].

Ultrasound synthesis of 1 as powder

To achieve **1** as powder, the ultrasonic probe was put into $Co(NCS)_2$ (10 mL, 0.1 M) while 2,5-dimethyl pyrazine (10 mL, 0.1 M) was drop-wisely added and repeated 4 times to study the effects of irradiation power, reactions temperature, and reactant concentration, as seen the table **3**. After filtering off, washing, and drying, analytical calculations were for $C_{26}H_{36}CoN_{10}O_2S_2$: Yield: 62%. calcd. C= 48.51, H =5.59, N =21.76, S =9.96%; found C =45.80, H =5.32, N =20.55, S =9.64%. IR (selected bands for **1**; in cm^{-1}): 3365(b), 3151(b), 2089(w), 1630(s), 1593(s), 1565(s).

RESULTS AND DISCUSSION

The reaction between the organic nitrogen-donor and oxygen donor-based 2,5-dimethyl pyrazine (L) and $Co(NCS)_2$ yielded crystalline material formulated as a new 0D coordination complex $[Co(NCS)_2(L)(H_2O)_2.3(L)]$ (**1**). Nano-structures of complex **1** were obtained in an aqueous solution by ultrasonic irradiation, while single crystals of complex **1**, suitable for X-ray crystallography, were prepared by a heat gradient applied to an aqueous solution of the reagents (the ‘‘branched tube method’’). Generally, the yield percentage of product **1** in the sonochemical method is higher than in the branch tube method. The most important reason can be related to the ultrasonic force as well as the heat produced by bursting the bubble in this method. This driving force will be a significant factor in increasing the yield percentage of **1**. But in the branched branch tube method, there is no such driving force.

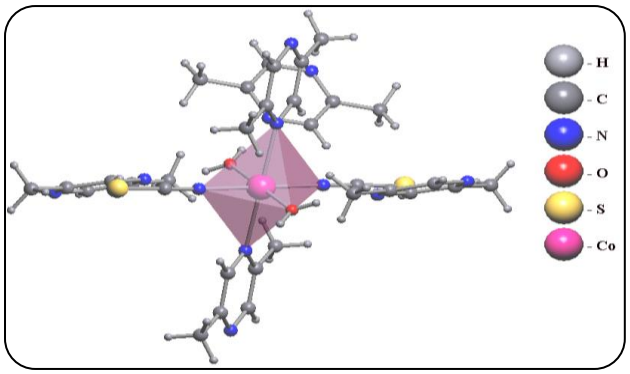

Fig. 1: Coordination around Co^{+2} cations

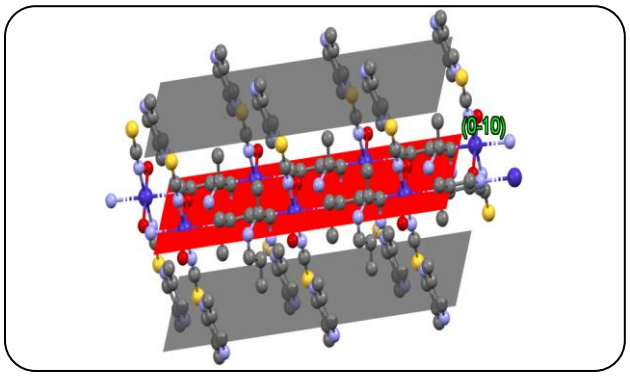

Fig. 2: Crystal packing along the [0-10] for 1

SCXRD output of **1** confirmed triclinic P_1^- space group. Additional crystallographic details are listed in Tables 1 and 2. Complex **1**: Two O atoms and four N atoms in octahedral coordination of O_2N_4 are coordinated to Co atoms (Fig. 1). One Co^{2+} coordinated to one 2,5-dimethyl pyrazine ligand (**L**), -NCS, one water molecule, and some parts of two others **L** are included in the asymmetric unit. However, two L ligands are present inside the crystal and aren't coordinated with Co^{2+} ions (Fig. S1). **L** is coordinated to Co^{2+} ion via through N atom of aromatic ring with (Co(1)–N(2) distance of 2.367 Å. In addition, two water molecules via Co-O bond are coordinated with Co–O distance of 2.059 Å (Table S1 and Fig. S2). Moreover, hydrogen bonding takes place among H of H_2O molecule, metal ions, and N (20) from **L**. Furthermore, two aromatic rings are distanced at 5.347 Å (Figs. S5 and S6). 0D coordination complexes of 1 are bridged through intramolecular interaction and the structure is extended via van der Waals and hydrogen bond interactions on 3D crystal packing (Fig. S5). Further, the crystal of **1** grows along the [0-10] directions (Fig. 2).

To compare the obtained materials produced via both methods, FT-IR spectra of **1** were provided in Fig. 3. It should be noted that to obtain FT-IR spectrum, elemental analysis,

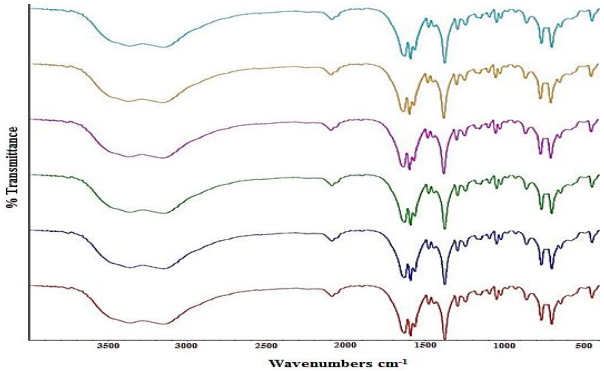

Fig. 3: The IR spectra of, 1-1 obtained by ultra-sonication (red line), 1- 2 (blue line), 1-3 (green line), 1-4 (pink line), 1-5 (brown line) as well as (simulated from SCXRD data of 1 (light blue line)

and PXRD, the 1-4 from ultrasonic samples were chosen since it has the smallest size among them. The stretching band of O-H from the H_2O molecule which is coordinated to Co atoms was located at 3365 cm^{-1}. Aromatic C-H stretching bands occurred near 3151 cm^{-1}. The absorption bands 2100 cm^{-1} resulted from the -NCS group and absorption bands around 1454 cm^{-1} related to CH_3 bending. The absorption bands with variable intensity in the frequency range 1400–1600 cm^{-1} correspond to ring vibrations of the pyrazine moiety of the ligand 2,5-dimethyl pyrazine. However, the stretching band assignment of the Co-O bond and Co-N bond stretching modes are coupling around 500 to 600 cm^{-1}. It can be suggested that both synthesizing procedures resulted in materials with inseparable elemental analysis and FT-IR data [52].

The simulated PXRD patterns of **1** generated using SCXRD data and the PXRD patterns of 1-1 to 1-4 samples produced through the process explained in the 2.3 section were compared in Fig. 4. As can be seen, their patterns are similar at the exact location of the 2θ diffractions confirming that the ultrasound-fabricated samples possess the same structure as a single crystal of 1.

Morphology and structure

Critical parameters that affect the morphology of **1** are ultrasonic power, the concentration of reactants, and the temperature of the reaction. The applied setting to produce sonicated samples were listed in Table 2. SEM images of sonicated samples (1-1 to 1-4), as shown in Fig. 5, examined their morphologies. It can be seen 1-1 and 1-3 samples have a micro-sized and uniform mixed morphology and 1-2, as well as 1-4 sample, have nano-sized

Table 2: Effects of ultrasonic power, concentration, time, and temperature on the morphology of 1

Entry	T (°C)[a]	t (min)[b]	Concentration (M)[c]	Sonication power (W)	Morphology (Mainly)
1-1	50	60	0.1	0	Mixed
1-2	50	60	0.1	60	Mixed
1-3	50	60	0.5	60	Mixed
1-4	70	60	0.1	60	Flakes

[a] Reaction temperature, [b] Reaction time, [c] Concentration of reactants.

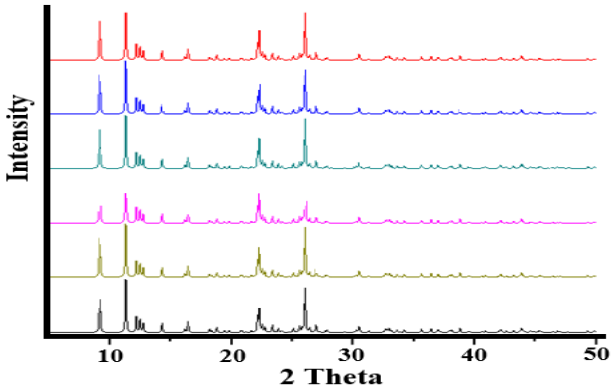

Fig.4: Powder XRD patterns of nano-sized 1-1 obtained by ultra-sonication (black line), 1- 2 (green line), 1-3 (pink line), 1-4 (bright blue), 1-5 (dark blue line) as well as (simulated from single-crystal X-Ray data of 1 (red line)

flakes. In Table 3 and Fig. 5, sample 1–1 was surveyed without power ultrasound and the other samples were studied under a variety of power ultrasound, concentration as well as temperature. To find out the role of power ultrasound irradiation on the character of the product, reactions were performed under completely different power ultrasound irradiation. In samples 1–1, the reaction was studied without power ultrasound. Results show that the size of particles sample 1–1 (Fig. 5b) is larger than 1–2 (Fig. 5a). Results show low power ultrasound irradiation decreased agglomeration and thus led to decreased particle size. Comparison between samples 1–2 and 1–3 shows an increase in nanoparticle size. Thus, the size particles of samples 1–3 are larger than 1–2 (Fig. 5b, c). Higher temperature (70 °C) results in an increased supersaturation of growth species in the solution, and thus particle size of samples 1–4 is larger than the particle size of samples 1–2 (Fig. 5b, d). The corresponding particle size distribution histogram of complex **1** nanoparticles has been shown in Fig. 5. It was found that the morphology of as-prepared, 1-1, 1-2, and 1-3 mixed morphology were not dependent on the reaction temperature, otherwise, 1-4 relied on the reaction temperature. According to obtained results, less agglomeration has occurred in samples 1-2 with controlled parameters as follows: irradiation power: 60 W, time: 60 min, concentration: 0.1 M, temperature: 50 °C (Table 2; Fig. 5b). Noteworthy, mixed morphology as 3D of the particles can be altered into small flaked as 2D by applying ultrasonic irradiation.

Hirshfeld surface analysis (HSA)

The Hirshfeld surface analyses of **1** have been done on its asymmetric unit. The views of the Hirshfeld surface mapped over d_{norm} (-0.5713 to 1.3535 Å), shape index (-1.000 to 1.000Å), and curvedness (-4.0000 to 0.4000) have been shown in Fig. 6.

The most prominent red spots on the d_{norm} surface of **1** are due to Co-N and Co-O bonds. In addition to, distinct blue spots around the aromatic ring of ligand are attributed to van der Waals interactions. Also, The C…H/H…C close contacts appear as very pale red spots or white areas. These contacts which are attributed to C-H…π interactions are visible as hollow orange areas (π…H) and bulging blue areas (H…π) on the shape index surface (Figs. 6 and 7).

The two-dimensional fingerprint plots of the sum of the contacts contributing to the Hirshfeld surface have been shown in Fig. 8, represented in normal mode. Complementary regions are visible in the fingerprint plots where one molecule acts as a donor (de > di) and the other as an acceptor (de < di). The highest share of the total Hirshfeld surface is related to H…H/H…H close contacts with 42.6%. The opposite relationship was exhibited for N···H/H···N interactions, which accounted for 18.9%. Furthermore, the extents of C···H/H···C and S···H/H···S interactions covered 16.4% and 12.9% of complex **1**. The most significant evidence for the stable presence of the crystal structures was the domination of these H-bonding contacts [53-55].

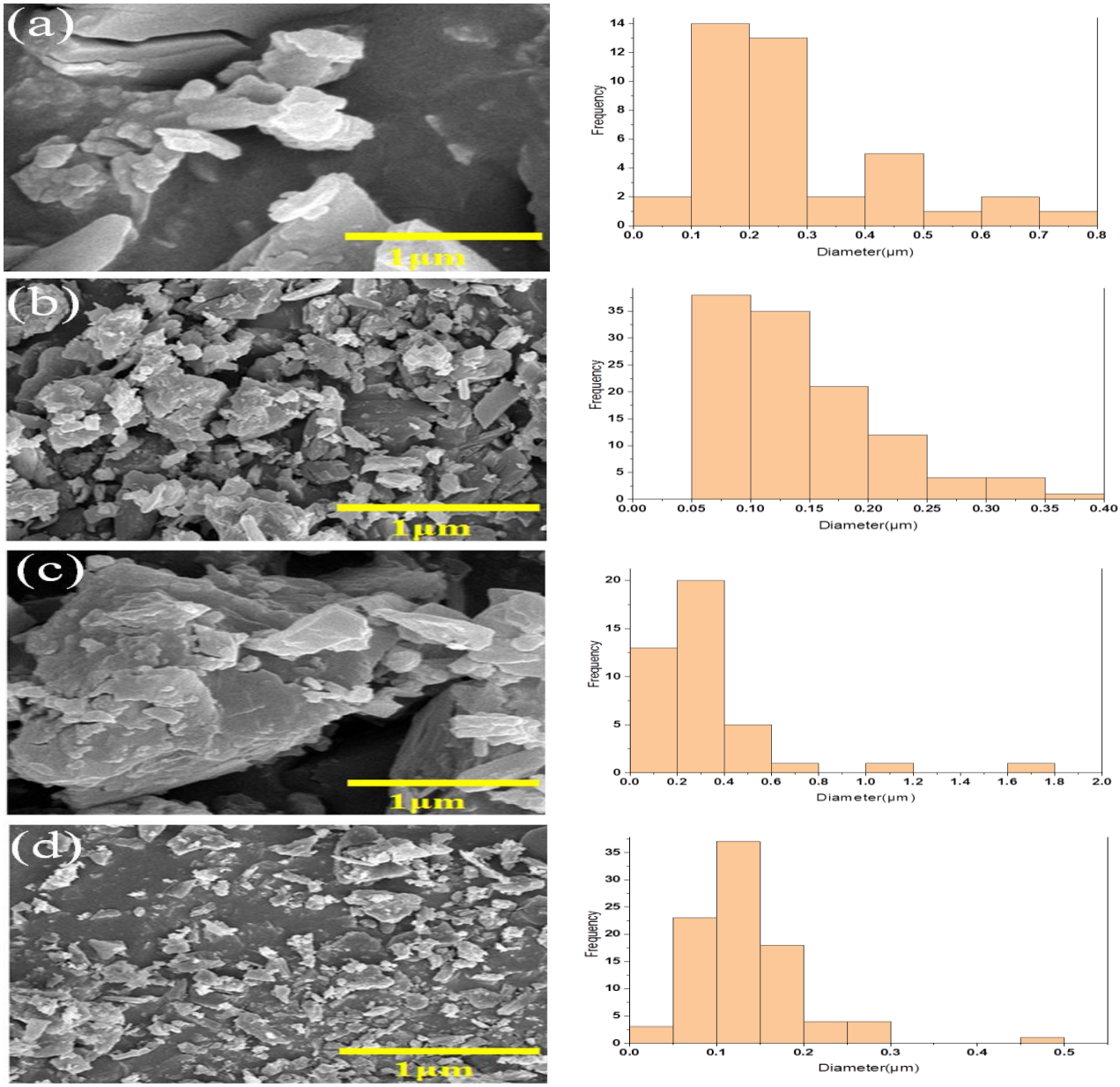

Fig. 5: SEM images and the corresponding particle size distribution histogram of micro- and nanosized particles: (a) 1-1 sample without sonication, (b) 1-2 sample with sonication (50 °C; 60 min; 0.1 M; sonication power: 60 W), (c) 1-3 sample (50 °C; 30 min; 0.1 M; sonication power: 60 W (d) 1-4 sample 70 °C; 60 min; 0.1 M; sonication power: 60 W)

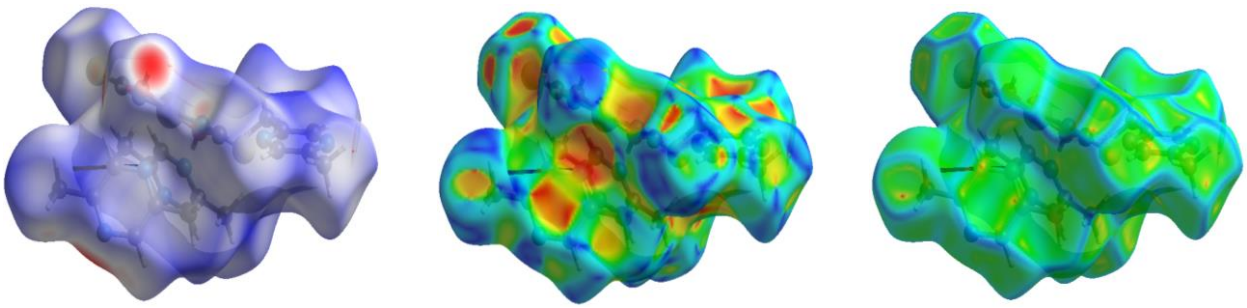

Fig. 6: Hirshfeld surfaces mapped with d_{norm}, shape index, and curvedness of 1

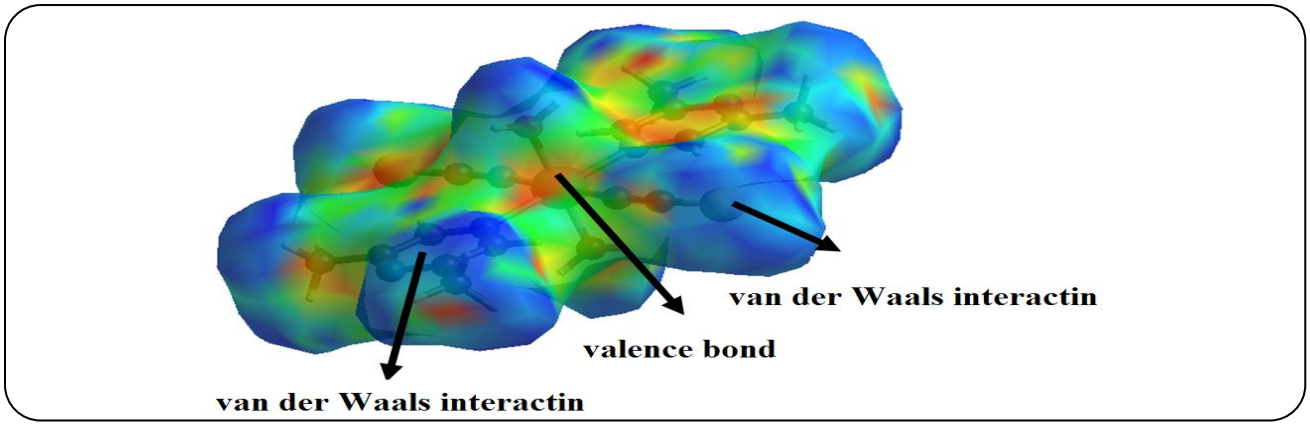

Fig. 7: Hirshfeld surface of 1

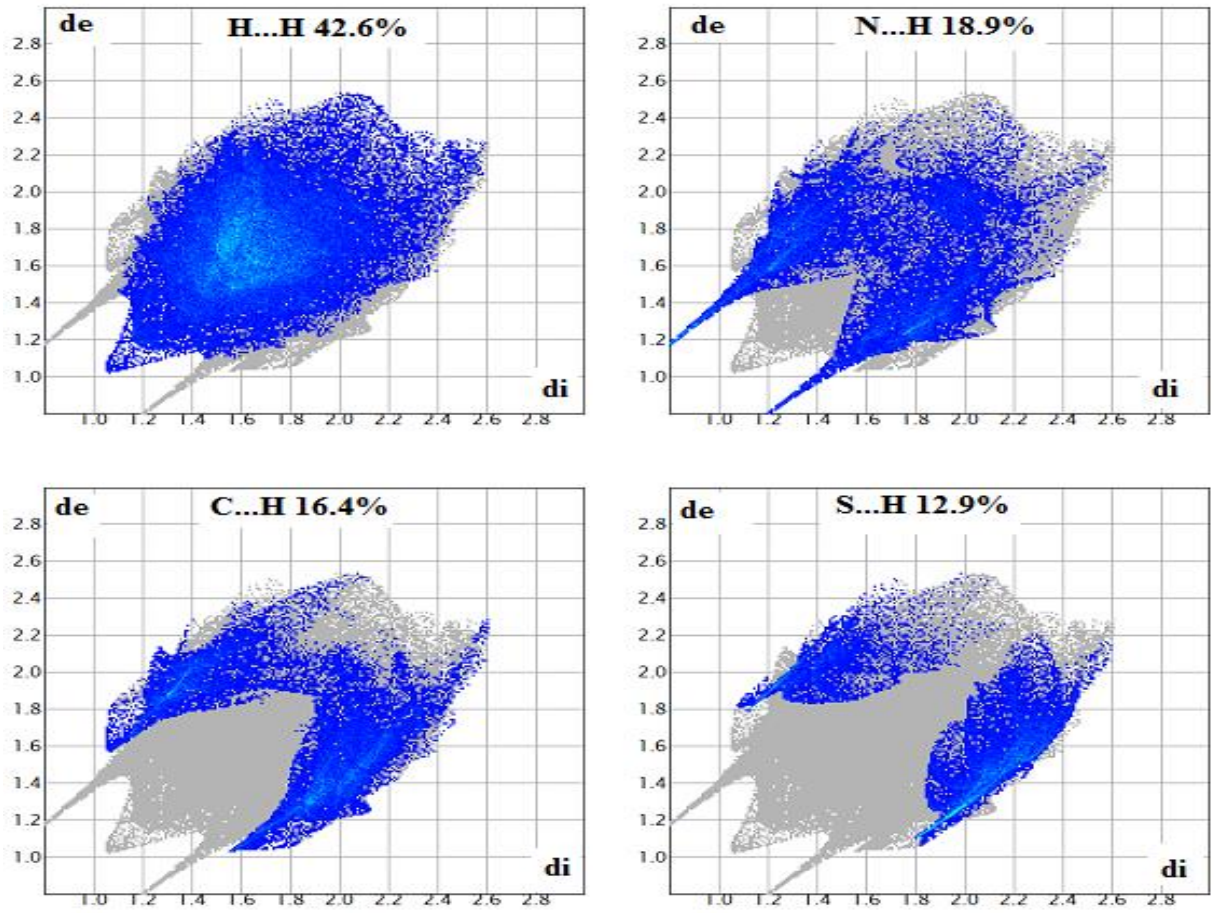

Fig. 8: 2-D fingerprint plots of 1

CONCLUSIONS

In the current research, novel nano Co-MOC (**1**) structures were synthesized and characterized using SEM, FT-IR, PXRD, and elemental analysis. Also, the quality of the obtained crystal by the branched tube method was in good condition which allowed it to be resolved by SCXRD. The crystal analysis of **1** exhibited Co^{2+} ions is six-coordinated. Furthermore, the powders obtained by the sonication ultrasound method were formed in the same crystalline phase as the one obtained from the branched tube method. The impacts of controlling parameters, i.e. temperature, ultrasound power, reactant concentration, and

time on morphology of **1** were also investigated and it was found that this technique has the potential to produce **1** as nanostructures. The optimum condition to produce smaller and less agglomerated nanosized particles of **1** was 50 °C, 60 min, 60 W, and 0.1 M. As a result, it can have a high potential to remove environmental pollutants, especially Persistent Organic Pollutants (POPs) through absorption and removal processes.

Acknowledgment

This research is the main part of my doctoral dissertation at the Department of Environmental Engineering of the Islamic Azad University (Hamedan Branch) and we thank the professors and instructors for their valuable comments and support, which have significantly improved the manuscript.

Received : Nov.15, 2022 ; Accepted : Feb.20, 2023

REFERENCES

[1] Liu F.C., Zeng Y.F., Li J.R., Bu X.H., Zhang H.J, Ribas J., Novel 3-D Framework Nickel (II) Complex with Azide, Nicotinic Acid, and Nicotinate (1−) as Coligands: Hydrothermal Synthesis, Structure, and Magnetic Properties, *Inorg. chem*., **44 (21)**: 7298-7300 (2005).

[2] Kanagathara N., MaryAnjalin F., Ragavendran V., Dhanasekaran D., Usha R., Rao R.G., Marchewka M.K., Experimental and Theoretical (DFT) Investigation of Crystallographic, Spectroscopic and Hirshfeld Surface Analysis of Anilinium Arsenate, *J. Mol. Struct*., **1223**: 128965 (2021).

[3] Moon D., Kang S., Park J., Lee K., John R.P., Won H., Seong G.H., Kim Y.S., Kim G.H., Rhee H., Lah M.S., Face-Driven Corner-Linked Octahedral Nanocages: M6L8 Cages Formed by C 3-Symmetric Triangular Facial Ligands Linked via C 4-Symmetric Square Tetratopic PdII Ions at Truncated Octahedron Corners, *J. Am. Chem. Soc.*, **128(11)**: 3530-3531 (2006).

[4] Naik I.K., Sarkar R., Madhu V., Bolligarla R., Kishore R., Das S.K., An Organic Receptor Isolated in an Unusual Intermediate Conformation: Computation, Crystallography, and Hirshfeld Surface Analysis, *J. Phys. Chem.*, **121(17)**: 3274-3286 (2017).

[5] Zhang L., Zhu Y., Nie Z., Li Z., Ye Y., Li L., Hong J., Bi Z., Zhou Y., Hu G., Co/MoC Nanoparticles Embedded in Carbon Nanoboxes as Robust Trifunctional Electrocatalysts for a Zn–Air Battery and Water Electrocatalysis, *ACS Nano*, **15(8)**: 13399-13414 (2021).

[6] Hayati P., Rezvani A.R., Morsali A., Retailleau P., Ultrasound Irradiation Effect on Morphology and Size of Two New Potassium Coordination Supramolecule Compounds. Ultrasonics Sonochemistry, *Ultrason Sonochem.*, **34**: 195-205 (2017).

[7] Karbul A., Mohammadi M.K., Yengejeh R.J., Farrokhian F., Synthesis and Characterization of Trimetallic Fe-Co-V/Zeolite and Fe-Co-Mo/Zeolite Composite Nanostructures, *Mater. Res.*, **24(3)**: e20200292 (2021).

[8] Shi Z., Wang Y., Lin H., Zhang H., Shen M., Xie S., Zhang Y., Gao Q., Tang Y., Porous NanoMoC@ Graphite Shell Derived from a MOFs-Directed Strategy: An Efficient Electrocatalyst for the Hydrogen Evolution Reaction, *J. Mater. Chem.*, **4(16)**: 6006-6013 (2016).

[9] Mehrdoost A., Jalilzadeh Yengejeh R., Mohammadi M.K., Babaei A.A, Haghighatzadeh A., Comparative Analysis of UV-assisted Removal of Azithromycin and Cefixime from Aqueous Solution Using PAC/Fe/Si/Zn Nanocomposite, *J. Health Sci. Surveill. Syst*., **9(1)**: 39-49 (2021).

[10] Jafarizadeh T., Hayati P., Neyrizi H.Z., Mehrabadi Z., Farjam M.H., Gutiérrez A., Adarsh N.N., Synthesis and Structural Characterization of a Novel Zn (II) Metal Organic Complex (Zn-MOC) and Elimination of Highly Consumed Antibiotic; Tetracycline from Aqueous Solution by their Nanostructures Photocatalyst under Visible Light, *J. Mol. Struct.*, **1228**: 129448 (2021).

[11] Liu C., Lin M., Fang K., Meng Y., Sun Y., Preparation of Nanostructured Molybdenum Carbides for CO Hydrogenation. RSC Advances, *RSC Adv.*, **4(40)**: 20948-54 (2014).

[12] Huseynova M., Ajdar M., Parham T., Mahizar A., Synthesis, Characterization, Crystal Structure of the Coordination Polymer Zn(II) with Thiosemicarbazone of Glyoxalic Acid and Their Inhibitory Properties Against Some Metabolic Enzymes, *Bioorg. Chem.*, **83**: 55-62 (2019).

[13]Sertçelik M., Çaylak Delibaş N., Çevik S., Necefoğlu H., Hökelek T., Poly [(μ5-2, 2′-bipyridine-5, 5′-dicarboxylato) lead (II)], *Acta Crystallogr Sect. E Struct. Rep. Online*. **68(9)**: m1196-7 (2012).

[14]Sertçelik M., Murat D., Synthesis, Characterization, and Antibacterial Activity of Cd (II) Complexes with 3-/4-Fluorobenzoates and 3-Hydroxypiridine as Co-Ligands, *Russ. J. Inorg. Chem.,* **65(9)**: 1351-1359 (2020).

[15] Sertçelik M., Synthesis, Spectroscopic Properties, Crystal Structures, DFT Studies, and the Antibacterial and Enzyme Inhibitory Properties of a Complex of Co (II) 3, 5-Difluorobenzoate with 3-Pyridinol, *Journal of Chemical Research,* **45(1-2)**: 42-48 (2021).

[16] Roesky H.W., Andruh M., The Interplay of Coordinative, Hydrogen Bonding and π–π Stacking Interactions in Sustaining Supramolecular Solid-State Architectures.: A Study Case of Bis (4-Pyridyl)-and Bis (4-Pyridyl-N-Oxide) tectons, *Coord. Chem. Rev.*, **236(1-2)**: 91-119 (2003).

[17] Ghosh D., Dhibar S., Dey A, Manna P., Mahata P., Dey B., A Cu (II)-Inorganic Co− Crystal as a Versatile Catalyst Towards 'Click'Chemistry for Synthesis of 1, 2, 3-Triazoles and β-Hydroxy-1, 2, 3-Triazoles, *Chemistry Select.*, **5(1)**: 75-82 (2020).

[18] Liu J., Guo Y., Fu X.Z., Luo J.L., Zhi C., Strengthening Absorption Ability of Co–N–C as Efficient Bifunctional Oxygen Catalyst by Modulating the d Band Center Using MoC, *Green Energy Environ.*, **8(2)**: 459-469 (2023).

[19] Batten S.R, Hoskins B.F, Robson R., Two Interpenetrating 3D Networks Which Generate Spacious Sealed-Off Compartments Enclosing of the Order of 20 Solvent Molecules in the Structures of Zn (CN)(NO3)(tpt) 2/3. Cntdot. Solv (Tpt= 2, 4, 6-Tri (4-Pyridyl)-1, 3, 5-Triazine, Solv=. Apprx. 3/4C2H2Cl4. Cntdot. 3/4CH3OH or. Apprx. 3/2CHCl3. Cntdot. 1/3CH3OH), *J. Am. Chem. Soc.*, **117(19)**: 5385-5386 (1995).

[20] Faramarzi R., Taheri A., Roushani M., Determination of Paraquat in Fruits and Natural Water using Ni(OH)2 Nanoparticles-Carbon Nanotubes Composite Modified Carbon Ionic liquid Electrode, *Anal. Bioanal. Electrochem.*, **7(6)**: 666-683 (2016).

[21] Jalilian R., Ezzatzadeh E., Taheri A., A Novel Self-Assembled Gold Nanoparticles-Molecularly Imprinted Modified Carbon Ionic Liquid Electrode with High Sensitivity and Selectivity for the Rapid Determination of Bisphenol A Leached from Plastic Containers, *J. Environ. Chem. Eng.*, **9(4)**: 105513 (2021) .

[22] Liu W., Sahoo B., Junge K., Beller M., Cobalt Complexes as an Emerging Class of Catalysts for Homogeneous Hydrogenations, *Acc. Chem. Res.*, **51(8)**: 1858-1869 (2018).

[23] Paritmongkol W., Sakurada T., Lee W.S., Wan R., Müller P., Tisdale W.A., Size and Quality Enhancement of 2D Semiconducting Metal–Organic Chalcogenolates by Amine Addition, *J. Am. Chem. Soc.*,**143(48)**: 20256-63 (2021).

[24] Lin W., Rieter W.J., Taylor K.M., Modular Synthesis of Functional Nanoscale Coordination Polymers, *Angew. Chem. Int. Ed.*, **48(4)**: 650-658 (2009).

[25] Spokoyny A.M, Kim D., Sumrein A., Mirkin C.A., Infinite Coordination Polymer Nano-and Microparticle Structures, *Chem. Soc. Rev.*, **38(5)**: 1218-1227 (2009).

[26] Bayati F., Mohammadi M.K, Yengejeh R.J., Babaei A.A., Ag_2O/GO/TiO_2 Composite Nanoparticles: Synthesis, Characterization, and Optical Studies, *J. Aust. Ceram.*, **57(1)**: 287-293 (2021).

[27] Bastami T.R., Khaknahad S., Malekshahi M., Sonochemical Versus Reverse-Precipitation Synthesis of CuxO/Fe_2O_3/MoC Nano-Hybrid: Removal of Reactive Dyes and Evaluation of Smartphone for Colorimetric Detection of Organic Dyes in Water Media, *Environ. Sci. Pollut. Res.*, **27(9)**: 9364-9381 (2020).

[28] Zad Z.R., Davarani S.S.H., Taheri A.R., Bide Y., Highly Selective Determination of Amitriptyline Using Nafion-AuNPs@branched Polyethyleneimine-Derived Carbon Hollow Spheres in Pharmaceutical Drugs and Biological Fluids, *Biosens. Bioelectron.*, **86:** 616-622 (2016).

[29] Babaei A., Aminikhah M., Taheri A.R, A Multi-Walled Carbon Nano-Tube and Nickel Hydroxide Nano-Particle Composite-Modified Glassy Carbon Electrode as a New Sensor for the Sensitive Simultaneous Determination of Ascorbic Acid, Dopamine and Uric Acid, *Sens. Lett.*, **11**: 413-422 (2013).

[30] Karimipour Z, Jalilzadeh Yengejeh R., Haghighatzadeh A., Mohammadi M.K., Mohammadi Rouzbehani M., UV-Induced Photodegradation of 2, 4, 6-Trichlorophenol Using Ag–Fe_2O_3–CeO_2 Photocatalysts, *J. Inorg. Organomet. Polym. Mater*., **31(3)**:1143-1152 (2021).

[31] Ghaemi A., Mohave F., Farhadi A., Takassi M.A., Tavakkoli H., Hydrothermal Synthesis of Mesoporous Cobalt Ferrite by Ionic Liquid-Assisted process; Catalytic Performance, Morphology, and Magnetic Studies, *J. Aust. Ceram.*, **57(4)**:1321-1330 (2021).

[32] Safarifard V., Morsali A., Joo S.W., Sonochemical Synthesis and Characterization of Nano-Sized Lead (II) 3D Coordination Polymer: Precursor for the Synthesis of Lead (II) Oxybromide Nanoparticles, *Ultrason. Sonochem.*, **20(5)**: 1254-1260 (2013).

[33] Paulusse J.M., Huijbers J.P., Sijbesma R.P., Quantification of Ultrasound-Induced Chain Scission in PdII–Phosphine Coordination Polymers, *Eur. J. Chem.*, **12(18)**: 4928-4934 (2006).

[34] Donoso G., Dominguez J.R., González T., Correia S., Cuerda-Correa E.M., Electrochemical and Sonochemical Advanced Oxidation Processes Applied to Tartrazine Removal. Influence of Operational Conditions and Aqueous Matrix, *Environ. Res.*, **202**: 111517 (2021).

[35] Haque E., Khan N.A, Park J.H, Jhung S.H., Synthesis of a Metal–Organic Framework Material, Iron Terephthalate, by Ultrasound, Microwave, and Conventional Electric Heating: a Kinetic Study, *Eur. J. Chem.*, **16(3)**: 1046-1052 (2010).

[36] Jung D.W., Yang D.A., Kim J., Kim J., Ahn W.S., Facile Synthesis of MOF-177 by a Sonochemical Method Using 1-Methyl-2-Pyrrolidinone as a Solvent, *Dalton Trans.*, **39(11)**: 2883-2887 (2010).

[37] Alavi M.A., Morsali A., Syntheses and Characterization of $Sr(OH)_2$ and $SrCO_3$ Nanostructures by Ultrasonic Method, *Ultrason. Sonochem.*, **17(1)**: 132-138 (2010).

[38] Kateshali A.F., Soleimannejad J., Sañudo E.C., Sonochemical Synthesis of Two Nanoscale Co (II) Coordination Compounds: Facile Fabrication of Co3O4 Nanoparticles with Various Morphologies, *Polyhedron*. **185**: 114565 (2020).

[39] Li J.X, Li Y.F, Liu L.W., Cui G.H., Luminescence, Electrochemical and Photocatalytic Properties of Sub-Micron Nickel (II) and Cobalt (II) coordination Polymers Synthesized by Sonochemical Process, *Ultrason. Sonochem.*, **41**: 196-205 (2018).

[40] Cui J.W., Li Y.H., Zhao L.Y., Cui G.H., Photoluminescence, Electrochemical Behavior and Photocatalytic Activities of Cobalt (II) Coordination Polymer Nanostructures Synthesized by Sonochemical Process, *Ultrason. Sonochem.*, **39**: 837-844 (2017).

[41] Bala R., Behal J., Kaur V., Jain S.K., Rani R., Manhas R.K., Prakash V., Sonochemical Synthesis, Characterization, Antimicrobial Activity and Textile Dyeing Behavior of Nano-Sized Cobalt(III) Complexes, *Ultrason. Sonochem.*, **35**: 294-303 (2017).

[42] Razmara Z., Janczak J., Sonochemical Synthesis and Structural Characterization of a New Three Mono-Nuclear Cobalt (II) Complex, to Produce Tricobalt Tetroxide as an Effective Heterojunction Catalyst, *Mol. Struct*, **1229**: 129500 (2021).

[43] Joharian M., Abedi S., Morsali A., Sonochemical Synthesis and Structural Characterization of a New Nanostructured Co (II) Supramolecular Coordination Polymer with Lewis Base Sites as a New Catalyst for Knoevenagel Condensation, *Ultrason. Sonochem.*, **39**: 897-907 (2017).

[44]Sheldrick G.M., SHELXT–Integrated Space-Group and Crystal-Structure Determination, *Acta Crystallogr. A.*, **1(1)**: 3-8 (2015).

[45] Spek A.L., Structure Validation in Chemical Crystallography, *Acta Crystallogr. D.*, **65**: 148–155 (2009).

[46] Nonius B., SADABS. Bruker Nonius, Delft, The Netherlands, 2002.

[47] Altomare A., Burla M.C., Camalli M., Cascarano G.L., Giacovazzo C., Guagliardi A., Moliterni A.G, Polidori G., Spagna R., SIR97: A New Tool for Crystal Structure Determination and Refinement, *J. Appl. Crystallogr.*, **32(1)**: 115-119 (1999).

[48] Spek A.L.J., Single-Crystal Structure Validation with the Program PLATON, *J. Appl. Crystallogr.*, **36(1)**: 7-13 (2003).

[49] Spackman P.R., Turner M.J., McKinnon J.J., Wolff S.K., Grimwood D.J., Jayatilaka D., Spackman M.A., CrystalExplorer: A program for Hirshfeld Surface Analysis, Visualization and Quantitative Analysis of Molecular Crystals, *J. Appl. Crystallogr.*, **54(3)**: 1006-1011 (2021).

[50] Chambers J.E., Migliorini F., MERCURY-A New Software Package for Orbital Integrations. InAAS/Division for Planetary Sciences Meeting Abstracts# 29, **29**: 27-06 (1997).

[51] Suckert S., Jess I., Näther C., Synthesis, Structures, and Thermal Properties of Cobalt(II) Thiocyanate Coordination Compounds with 2, 5-Dimethylpyrazine, *Z Anorg Allg Chem.*, **643(11)**: 721-728 (2017).

[52] Vetrivelan V., Spectra, Electronic Properties, Biological Activities and Molecular Docking Investigation on Sulfonamide Derivative Compound: An Experimental and Computational Approach, *J. Nanosci. Nanotechnol.*, 348-352 (2022).

[53] Li C.G., Chai Y.M., Chai L.Q., Xu L.Y., Novel Zinc (II) and Nickel (II) Complexes of a Quinazoline-Based Ligand with an Imidazole Ring: Synthesis, Spectroscopic Property, Antibacterial Activities, Time-Dependent Density Functional Theory Calculations and Hirshfeld Surface Analysis, *Appl. Organomet. Chem.*, **36(5)**: e6622 (2022).

[54] Tyula Y.A., Zabardasti A., Goudarziafshar H., Kucerakova M., Dusek M., A New Supramolecular Zinc (II) Complex Containing 4-Biphenylcarbaldehyde Isonicotinoylhydrazone Ligand: Nanostructure Synthesis, Catalytic Activities and Hirshfeld Surface Analysis, *Appl. Organomet. Chem.*, **32(3)**: e4141 (2018).

[55] Chai Y.M., Li C.G., Zhang X.F., Chai L.Q., Antimicrobial Activities of two 1-D, 2-D, and 3-D Mononuclear Mn (II) and Dinuclear Bi (III) Complexes: X-Ray Structures, Spectroscopic, Electrostatic Potential, Hirshfeld Surface Analysis, and Time-Dependent/Density Functional Theory Studies, *Appl. Organomet. Chem.*, **36(6)**: e6682 (2022).